Journal of Alloys and Compounds, 184 (1992) 275–284
JALCOM 195

Pyrite-type $RuS_{2-2x}Se_{2x}$ and $Ru_{1-x}Os_xS_2$ solid solutions: X-ray structure determination and Raman spectra*

Th. Stingl, B. Müller and H. D. Lutz
Universität Siegen, Anorganische Chemie I, Postfach 101240, W-5900 Siegen (FRG)

(Received November 27, 1991)

Abstract

X-ray structure determination and Raman spectra of $RuS_{2-2x}Se_{2x}$ and $Ru_{1-x}Os_xS_2$ single crystals grown by the chemical vapour transport technique and tellurium fluxes respectively are presented and discussed with respect to the nature of the solid solutions, possible superstructure ordering and lattice dynamics. In the case of $RuS_{2-2x}Se_{2x}$, contrary to $NiS_{2-2x}Se_{2x}$, only homonuclear S_2 and Se_2 units are present: these probably order, forming cobaltite-type domains. The Raman-allowed modes, which show two-mode behaviour, reflect the change in the lattice forces with increasing x. In the pyrite-type $Ru_{1-x}Os_xS_2$, there is a random distribution of the metal ions. Both the S–S bond lengths and the SS stretching modes reveal Vegard's rule-like behaviour. The S_2 librations, however, are sensitive to the local environment of the S_2 units in the $Ru_{6-x}Os_xS_2$ clusters.

1. Introduction

In the scope of lattice dynamics and bonding in compounds with dumbbell-like anionic units X_2 (X≡S, Se, Te; P, As, Sb), we are concerned with binary pyrite-type compounds MX_2 $cP12$ (space group, $Pa\bar{3}$) [1–4]. In the case of ternary compounds such as $M_{1-x}M'_xX_2$ or $MX_{2-2x}X'_{2x}$, the question arises whether the properties smoothly change with increase in x or whether clusters or superstructures are formed. Thus, for $MX_{2-2x}X'_{2x}$, solely X_2 and X'_2 units or additionally XX′ units may be present in structure. In the case of ternary MXY (X≡S, Se, Te; Y≡P, Se, Sb), all possibilities have been established, namely solely homonuclear units (*e.g.* cobaltite (CoAsS)), only heteronuclear anions (*e.g.* gersdorffite (NiAsS)), all X_2, XY and Y_2 (*e.g.* ullmannite (NiSbS)) [5].

We therefore have grown single crystals of the series $RuS_{2-2x}Se_{2x}$ and $Ru_{1-x}Os_xS_2$ and performed single-crystal X-ray structure determinations [6] and single-crystal Raman experiments [3]. As known from previous work [7], pyrite-type RuS_2 and $RuSe_2$ form a complete series of solid solutions obeying Vegard's rule. This is also true for $Ru_{1-x}Os_xS_2$. In the case of $NiS_{2-2x}Se_{2x}$, Lemos *et al.* [8] revealed from Raman single crystal spectra that SSe units are formed in addition to S_2 and Se_2 units. We now confirm these results (see below).

*Dedicated to Professor Rudolf Hoppe on the occasion of his 70th birthday.

0925-8388/92/$5.00

2. Preparation of single crystals

Single crystals of $RuS_{2-2x}Se_{2x}$ and $Ru_{1-x}Os_xS_2$ were grown by the chemical vapour transport technique using ICl_3 as the transporting agent and from tellurium fluxes respectively (Table 1). In the case of $RuS_{2-2x}Se_{2x}$, the selenium content of the crystals grown was smaller than that of the starting material. For further details see ref. 3.

The composition of the single crystals grown was determined from the unit-cell dimensions calculated from X-ray Guinier powder data (Cu $K\alpha_1$ radiation; α-quartz as internal standard; least-squares refinement). In the case of $Ru_{1-x}Os_xS_2$, however, an X-ray structure determination (see below) had to be performed because the lattice constants of RuS_2 and OsS_2 with $a = 561.06(3)$ pm [9] and 561.94(7) pm [6] are too similar.

2.1. X-ray structure determination

Approximately spherical crystals were transferred to an Enraf–Nonius CAD 4 diffractometer. Graphite-monochromatized Mo $K\alpha$ radiation was used. The intensity data were corrected for Lorentz and polarization effects with NRCVAX [10] and SDP [11] respectively. Spherical absorption corrections were performed by using the absorption correction factors given in ref. 12. The variations in intensity throughout the data collection were less than 1%. The structures were refined by full-matrix least-squares refinement of positional anisotropic thermal parameters, occupation factors, extinction coefficients and scale factors using scattering factors for neutral atoms [12] including the terms of anomalous dispersion. Initial parameters for the atomic positions

TABLE 1

Preparation of single crystals of pyrite-type $RuS_{2-2x}Se_{2x}$ and $Ru_{1-x}Os_xS_2$

x	Temperature (°C)	Crystal size (mm^3)
$RuS_{2-2x}Se_{2x}$ (vapour transport, ICl_3)[a]		
0.23	1120–1090	0.4×0.4×0.4
0.25	1120[b]	0.6×0.6×0.6
0.26	1120–1070	0.5×0.5×0.5
0.52	1120–1092	0.2×0.2×0.2
0.73	1120[b]	1×1×1
0.77	1120[b]	0.3×0.3×0.3
$Ru_{1-x}Os_xS_2$ (Te flux)[c]		
0.20	1000	0.4×0.7×0.7
0.362	1000	0.7×0.7×0.7
0.50	1000	1.0×0.7×0.7
0.638	1000	0.5×0.5×0.7

[a]Growing time, 25 days.
[b]Crystals have grown at the surface of the starting material.
[c]Alumina crucible in quartz-glass ampoules.

TABLE 2

Crystallographic data and data of structure refinement

	$RuS_{1.54}Se_{0.46}$	$Ru_{0.64}Os_{0.36}S_2$	$Ru_{0.36}Os_{0.64}S_2$
Lattice constant (pm)	568.04(7)	561.35(7)	561.60(7)
$F(000)$	337	350	385
Absorption coefficient (cm^{-1})	185.9	337.1	505.8
θ (°)	1–50	1–50	1–50
Ranges of $h\,k\,l$	$-12<h,k,l<+12$	$-10<h,k,l<+10$	$-10<h,k,l<+10$
Standard reflections	606, 206, 424	606, 260, 424	660, 062, 080
Measured reflections	969	862	916
Observed reflections	847	709	733
Unique reflections	330	293	313
Reflections included	304	241	263
Cut-off	$I>3\sigma_I$	$I>3\sigma_I$	$I>3\sigma_I$
Variables	6	7	7
R values (R, R_w) (%)	4.3, 4.4	1.5, 1.7	2.6, 2.9
S	3.2	0.8	4.0
Extinction coefficients	± 0	1.04(4)	1.11(5)

were interpolated from data in the literature on the binary compounds and for mean thermal parameters from the Wilson diagram. The crystallographic data and data of structure refinement are given in Table 2.

2.2. Raman measurements

The Raman spectra were recorded on a Dilor Omars 89 multichannel Raman spectrograph with the backscattering technique. For excitation the 676.4 and 647.1 nm radiation of a Kr^+ ion laser as well as the 514.5 and 488 nm radiation of an Ar^+ ion laser were used. The spectral slit widths are 3 cm^{-1} and 5 cm^{-1} respectively. For more details (recording parameters, calibration, measuring geometries etc.) see refs. 1–3.

3. Results

3.1. Crystal structure

The structure data of $Ru_{1-x}Os_xS_2$ and $RuS_{1.54}Se_{0.46}$ obtained are shown in Tables 3 and 4.

In the case of $Ru_{1-x}Os_xS_2$, there are solid solutions with pyrite structure and random distribution of the metal ions. Because of the strong correlation between the parameters refined [6] the composition of the mixed crystals was determined by refinement of the scale factor, positional parameters of S, and the occupation factor of the metal ion site. In the final refinement, the occupation factors obtained were fixed. The intraionic S–S distances, which increase on going from RuS_2 to OsS_2, obey Vegard's rule.

For $RuS_{1.54}Se_{0.46}$, the composition can be obtained from the unit-cell dimensions. Assuming Vegard's rule to be obeyed also for the intraionic X–X

TABLE 3

Fractional atomic coordinates with estimated standard deviations in parentheses and anisotropic temperature factors U_{ij} (space group, $Pa\bar{3}$)

	Site	x, y, z	u_{11} ($\times 10^2$ pm^2)	u_{12} ($\times 10^2$ pm^2)
$RuS_{1.54}S_{0.46}$				
Ru	4a	0	6.7(1)	−0.01(1)
S, Se	8c	0.38601(12)	6.8(2)	0.05(2)
$Ru_{0.64}Os_{0.36}S_2$				
Ru, Os	4a	0	2.14(15)	−0.07(4)
S	8c	0.38762(8)	3.06(17)	0.12(17)
$Ru_{0.36}Os_{0.64}S_2$				
Ru, Os	4a	0	2.41(11)	−0.06(3)
S	8c	0.38705(9)	3.52(17)	0.24(17)

$u_{11}=u_{22}=u_{33}$; $u_{12}=u_{13}=u_{23}$.

TABLE 4

Interatomic distances (X≡S, Se)

		Interatomic distance (pm)		
		$RuS_{1.54}Se_{0.46}$	$Ru_{0.64}Os_{0.36}S_2$	$Ru_{0.36}Os_{0.64}S_2$
X–X	1×	224.30(7)	218.52(2)	219.74(4)
$X_2\cdots X_2$	6×	323.33(4)	320.39(7)	320.23(8)
	6×	348.30(5)	344.34(4)	344.44(4)
$M–X_2$	2×	379.79(6)	376.88(11)	376.49(12)
$M–X_2$	6×	237.62(5)	235.17(6)	235.15(4)
$M–X_2$	6×	360.59(4)	355.15(9)	355.73(10)

distance this bond length should be 223.3 pm instead of 224.3 pm. Because in both single-crystal and powder X-ray photographs, weak reflections not allowed in the space group $Pa\bar{3}$ structure have been observed, refinement in the space group $P2_1/c$ (cobaltite type [13]) was also performed (Table 5). However, the R values obtained (R_w=5.9% instead of 4.4%) become worse and the occupation factors of the two anion sites differ only slightly. The structure data equal those of refinement in the space group $Pa\bar{3}$. Refinement of the X-ray data in the orthorhombic space group $Pca2_1$ also claimed for cobaltite [15, 16] results in an R value of only 6.5% without separating the S_2 and Se_2 units [6].

3.2. Raman spectra

Single-crystal Raman spectra of $Ru_{1-x}Os_xS_2$ pyrite-type solid solutions are shown in Fig. 1, and those of $RuS_{2-2x}Se_{2x}$ in Fig. 2 (see also ref. 3). The Raman scattering peaks observed are given in Table 6.

TABLE 5

Structure refinement of $RuS_{1.54}Se_{0.46}$ in space group $P2_1/c$ (see Table 3)

	Site	x	y	z	u_{11} ($\times 10^2$ pm^2)	u_{22} ($\times 10^2$ pm^2)	u_{33} ($\times 10^2$ pm^2)	u_{12} ($\times 10^2$ pm^2)	u_{13} ($\times 10^2$ pm^2)	u_{23} ($\times 10^2$ pm^2)
Ru(1)	2a	0	0	0	4.7(3)	4.1(2)	5.3(3)	−0.2(2)	3.1(4)	−0.2(2)
Ru(2)	2d	0.5	0.5	0	5.3(3)	4.1(2)	5.5(3)	−0.1(1)	2.7(4)	0.1(2)
S, Se(1)	4e	0.8859(3)	0.3865(2)	0.1143(3)	4.4(6)	4.6(4)	5.1(6)	0.4(4)	4.3(6)	−0.5(4)
S, Se(2)	4e	0.6137(3)	0.8854(3)	0.1142(3)	6.3(6)	4.1(4)	7.0(6)	−0.1(4)	0.4(7)	−0.7(4)

$a = 568.22(7)$ pm; $b = 568.15(7)$ pm; $c = 568.29(7)$ pm; $\beta = 89.95°(7)$; $R = 5.4\%$; $R_w = 5.9\%$.

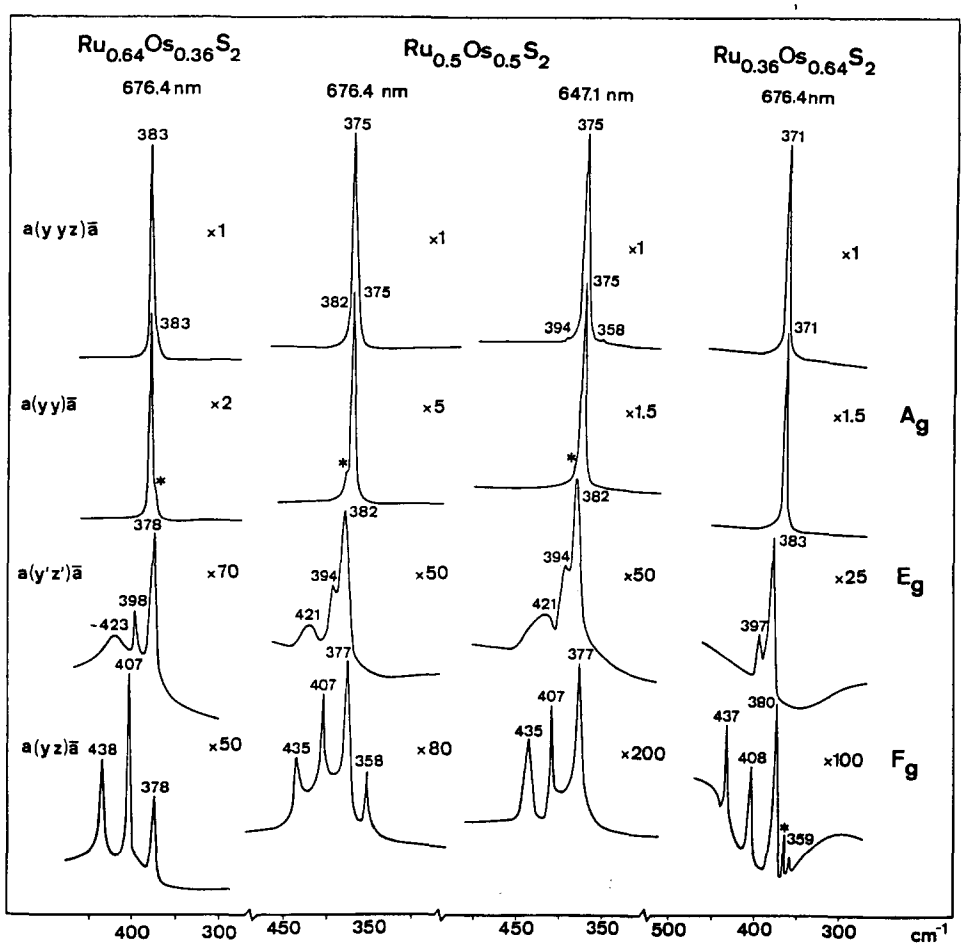

Fig. 1. Single-crystal Raman spectra of $Ru_{1-x}Os_xS_2$ pyrite-type solid solutions excited by 647.1 and 676.4 nm radiation. Measuring geometries are given using the notation of Damen *et al.* [14]: *y y z* means spectra recorded without the use of polarization analysers; asterisks indicate incomplete extinctions; $\times n$ is the ordinate scaling factor.

For $Ru_{1-x}Os_xS_2$ pyrite-type mixed crystals, only one band of species A_g but, contrary to group theory ($\Gamma = A_g + E_g + 3F_g + \ldots$; unit-cell group, T_h), up to three (?) and four peaks of species E_g and F_g have been observed. This means that the SS stretching modes of species A_g [1, 3] reveal one-mode behaviour, and the S_2 librations of species E_g and F_g two-mode behaviour.

In the case of $RuS_{2-2x}Se_{2x}$ solid solutions, it is undoubtedly revealed that, unlike $NiS_{2-2x}Se_{2x}$ [8], only S_2 and Se_2, but not SSe units are present. This is shown from Raman scattering peaks of species A_g, *i.e.* 391–336 cm^{-1} (S_2) and 233–272 cm^{-1} (Se_2). The corresponding mode frequencies of $NiS_{1.2}S_{0.8}$ are 447 cm^{-1} (S_2) and 263 cm^{-1} (Se_2), and that of the SSe units 360 cm^{-1}. The Raman bands of $RuS_{1.05}Se_{0.95}$ can be assigned to unit-

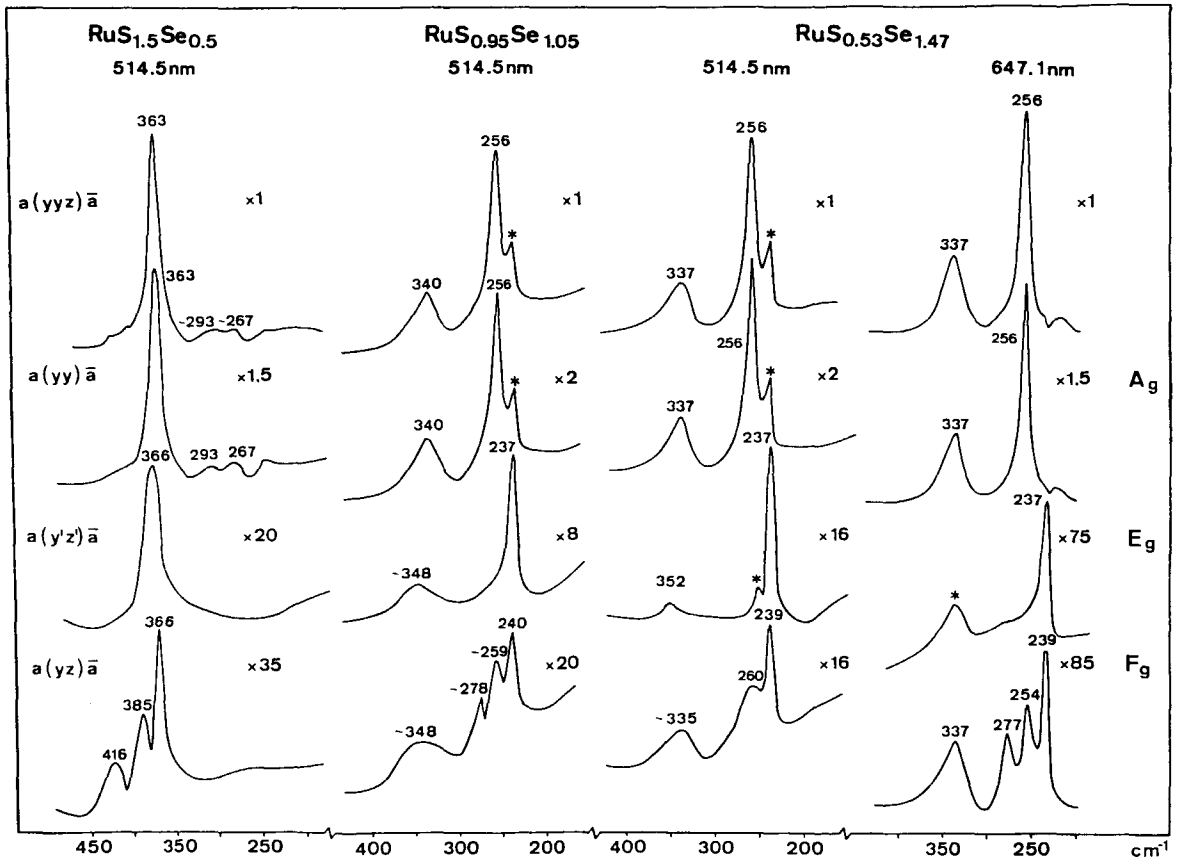

Fig. 2. Single-crystal Raman spectra of $RuS_{2-2x}Se_{2x}$ (for further explanations see Fig. 1).

TABLE 6

Raman scattering peaks of pyrite-type $RuS_{2-2x}Se_{2x}$ and $Ru_{1-x}Os_xS_2$

x	Peak (cm^{-1}) for the following species		
	A_g	E_g	F_g
$RuS_{2-2x}Se_{2x}$			
0	391	377	440, 409, 379
0.2	365	369	420, 388, 367
0.25	363, 267	366	416, 385, 360
0.52	340, 256	348, 237	348, 278, 259, 240
0.73	337, 256	352, 237	337, 277, 254, 239
0.77	336, 256	263, 234	345, 283, 259, 239
1.00	233	221	273, 244, 224
$Ru_{1-x}Os_xS_2$			
0	391	377	440, 409, 379
0.20	386	374	441, 407, 377, 353
0.36	383	423, 398, 378	438, 407, 378
0.5	375	421, 394, 382	435, 407, 377, 358
0.64	371	397, 383	437, 408, 380, 359
1.0	354	393	457, 411, 373

The species A_g, E_g and F_g are with respect to unit-cell group T_h (space group, $Pa\bar{3}$).

TABLE 7

Assignment of the Raman bands of $RuS_{0.95}Se_{1.05}$ with respect to space group $P2_1/c$ of the cobaltite structure (unit-cell group, C_{2h}; see text)

A_g				B_g			
ν_{ss}	ν_{SeSe}	R_{S_2}	R_{Se_2}	ν_{ss}	ν_{SeSe}	R_{S_2}	R_{Se_2}
340	256	348, 385[a]	237, 259	348	278	360[a]	240

The correlation of point group T_h to C_{2h}: $A_g \rightarrow A_g$, $E_g \rightarrow 2A_g$, $F_g \rightarrow A_g + 2B_g$. [a]Bands observed for $RuS_{0.5}Se_{1.5}$ (see Table 6).

cell group modes of the cobaltite structure (space group, $P2_1/c$) ($\Gamma = 6A_g + 6B_g + 11A_u + 10B_u$; unit-cell group, C_{2h}) without any exception (Table 7). Thus eight of the 12 Raman-allowed modes are observed. (For space group $Pca2_1$ (see above), 32 modes would be allowed with the Raman experiment [17].) IR spectra of powdery compounds with very broad bands indicating great disorder have been given in ref. 7.

4. Discussion

4.1. Cobaltite-type RuSSe and $RuS_{2-2x}Se_{2x}$ solid solutions

The Raman data confirm (or at least they are not inconsistent with) the assumption that the S_2 and Se_2 dumbbell-like units present in RuSSe are

ordered as in the cobaltite structure with the monoclinic space group $P2_1/c$. We assume that the small separation established by refinement in $P2_1/c$ (see Table 5) does not reflect the real separation and rather domains of (more or less fully separated) cobaltite-type structure are present in RuSSe.

Because of the presence of only S_2 and Se_2 units the Raman bands of $RuS_{2-2x}Se_{2x}$ solid solutions (with $x \neq 0$, 0.5 and 1) show two-mode behaviour. The modes observed are shifted to lower wavenumbers with increase in x because of the decrease in the lattice forces with increasing size of the unit cell.

4.2. Pyrite-type $Ru_{1-x}Os_xS_2$ mixed crystals

Lattice dynamics and bonding of RuS_2 and OsS_2 differ strongly. This has already been shown by the different nature of the Raman modes observed. Thus the frequencies of the respective bands range from ν_{SS} (stretching vibrations) $> R_{S_2}$ (librations) for RuS_2, but $\nu_{SS} < R_{S_2}$ for OsS_2, reflecting the much stronger metal–sulphur bonds of OsS_2 than those of RuS_2 [1]. This behaviour strongly complicates the interpretation of the spectra of the solid solutions, especially in the case of species F_g with both stretching and librational modes.

The SS stretching modes of species A_g (one-mode behaviour) reveal Vegard's rule-like behaviour and hence are shifted to lower wavenumbers with increase in osmium content (see Fig. 3). These findings mean that the intraionic S–S bonds are influenced by the total interionic lattice forces rather than by the actual local $Ru_{6-x}Os_x$ environment of the S_2 ion. The vibrational mode of the stretching vibration of species F_g obviously changes to those of S_2 librations with increase in x without any larger frequency shifts. The E_g mode of the pyrite structure (pure S_2 libration) reveals a two-mode

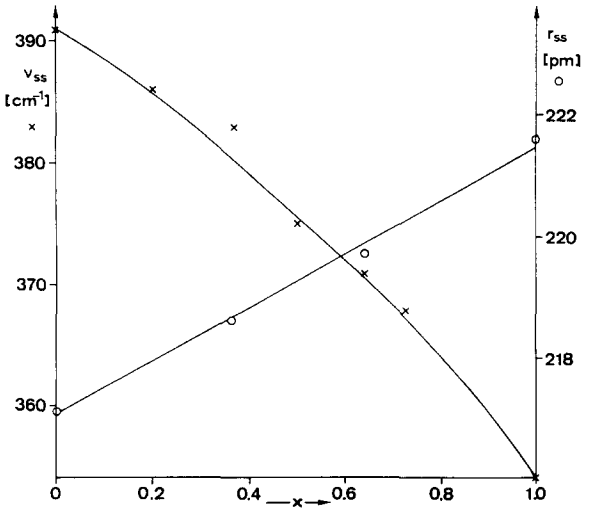

Fig. 3. Decrease in SS stretching frequencies and increase in S–S bond lengths with increase in x for $Ru_{1-x}Os_xS_2$ pyrite-type solid solutions.

behaviour (see Fig. 1). It is obviously more sensitive to the nature of the local $Ru_{6-x}Os_xS_2$ clusters, probably in such a manner that the S_2 librations split in one with preferential S_2–Os interaction (393–398 cm^{-1}) and in the other with S_2–Ru interaction (377–382 cm^{-1}).

References

1 B. Müller and H. D. Lutz, *Phys. Chem. Miner.*, *17* (1991) 716.
2 B. Müller and H. D. Lutz, *Solid State Commun.*, *78* (1991) 469.
3 B. Müller, *Thesis*, University of Siegen, 1990.
4 H. D. Lutz, J. Himmrich, B. Müller and G. Schneider, *J. Phys. Chem. Solids*, (1991), in the press.
5 A. F. Wells, *Structural Inorganic Chemistry*, 5th edn., Oxford University Press, Oxford, 1986, p. 760.
6 Th. Stingl, *Thesis*, University of Siegen, 1991.
7 P. Willich, *Thesis*, University of Köln, 1975.
8 V. Lemos, G. M. Gualberto, J. B. Salzberg and F. Cerdeira, *Phys. Status Solidi B*, *100* (1980) 755.
9 H. D. Lutz, B. Müller, Th. Schmidt and Th. Stingl, *Acta Crystallogr., Sect. C*, *46* (1990) 2003.
10 E. J. Gabe, F. L. Lee and Y. LePage, *The NRCVAX Crystal Structure System, Crystallographic Computing 3*, Clarendon, Oxford, 1985.
11 B. A. Frenz & Associates, Inc., *SDP Structure Determination Package*, College Station, TX; Enraf–Nonius, Delft, 1988.
12 *International Tables for X-ray Crystallography*, Vol. II, 1972; Vol. IV, 1974.
13 E. Onorato, *Acta Crystallogr.*, *10* (1957) 764.
14 T. G. Damen, S. P. S. Porto and B. Tell, *Phys. Rev.*, *144* (1966) 771.
15 R. F. Giese and P. F. Kerr, *Am. Mineral.*, *50* (1965) 1002.
16 H. Nahigian, J. Steger, H. L. McKinzie, R. J. Arnott and A. Wold, *Inorg. Chem.*, *13* (1974) 1498.
17 G. Kliche, *Thesis*, University of Siegen, 1979.